Mean-field model for the dynamics of conductance-based networks of excitatory and inhibitory spiking neurons with adaptation

Matteo di Volo,[1] Alberto Romagnoni,[2,3] Cristiano Capone,[4] and Alain Destexhe[1,4]

[1] *Unité de Neuroscience, Information et Complexité (UNIC), CNRS FRE 3693, 1 avenue de la Terrasse, 91198 Gif sur Yvette, France*

[2] *Centre de recherche sur l'inflammation UMR 1149, Inserm - Université Paris Diderot*

[3] *Data Team, Département d'informatique de l'ENS, École normale supérieure, CNRS, PSL Research University, 75005, Paris, France*

[4] *European Institute for Theoretical Neuroscience, 74 Rue du Faubourg Saint-Antoine, Paris, 75012 France*

(Dated: June 20, 2018)

Cortical networks are composed of excitatory and inhibitory cells interconnected through conductance-based synaptic interactions, and characterized by spike frequency adaptation in a large number of cells. We report here a mean-field model of such networks using adaptive exponential integrate and fire spiking neurons, taking explicitly into account adaptation. We first show that the mean-field model is capable to correctly predict the average spontaneous activity states in asynchronous irregular regimes. Next, we show that the mean-field model is able to capture the transient temporal response of the network at a global scale, driven by adaptation dynamics. Finally, we show that the mean-field model can also capture the dynamics of the system in a regime where high and low activity states alternate (UP-DOWN state dynamics), where adaptation is critical to define the bistable properties of the system, leading to slow oscillations. We conclude that the mean-field model with adaptation can capture the mean level of activity, the responsiveness and the oscillatory dynamics of conductance-based networks of excitatory and inhibitory cells.

I. INTRODUCTION

The dynamical regimes observed experimentally in cerebral cortex range from asynchronous states, typically in wakefulness, to regimes displaying slow oscillations consisting of alternating high and low activity states (UP and DOWN states), typically in slow-wave sleep [1–5]

These states have a common ground of an irregular spiking activity of single neurons [6], while their interaction is known to be mediated by conductance-based synapses [7]. The role of irregularity in neurons activity has been proposed to be important for neurons responsiveness and learning [8]. Because of this feature, the typical asynchronous state observed during awake animals recording is usually named as asynchronous irregular (AI).

Conductances have been observed to play a key role in network response to external input, as the state of the system can have different outputs to the same specific stimuli [9]. Accordingly, these features should be taken into account in order to deal with a physiologically realistic model of the brain cortex.

While the implementation of spiking network models able to satisfy these characteristics is relatively simple and has been performed in the literature [10, 11], the derivation of a dimensionally reduced mean-field model of this system is not straightforward because of the difficulties in treating adaptation and conductance-based synapses.

Some attempts have been done in the literature based mainly on LIF neurons, according to an approximations of the neurons transfer functions TF (i.e. the output firing rate of a single neuron in function of its inputs). Phenomenological approaches, based on the assumption of a linear transfer function, have been used in [12] in order to reproduce the rate response of the network. A solid theoretical bottom-up approach for obtaining mean field equations in AI regimes has been performed in [13]. Let us notice that, at variance with many other approaches, this mean field formulation permits to predict both average population rates and also covariance between different population activities. According to this formalism, mean field equations giving access to network temporal dynamics can be obtained once the neurons stationary TF (i.e. the neuron response to stationary external input) is obtained. In that paper, as in [12], an approximation for the TF has been obtained for LIF neurons.

Nevertheless, more realistic cellular models are necessary to reproduce cells spiking activity in the cortex. In particular, the adaptive exponential (AdEx) integrate and fire model has been found to provide a good level of realism for modeling inhibitory FS-cell (with zero or small adaptation) and excitatory RS-cell (with higher adaptation) as observed in the cortex [14–16].

However, despite its realism, there is no analytic TF for the conductance based AdEx model, which complicates the construction of mean-field models. Recently, a semi-analytical approach was proposed [17] for the calculation of the TF of AdEx neurons, which could be potentially applicable to any neuron model and, more interestingly, to experimental data about single cell activity [18]. This approach allowed us to build a mean-field model of AdEx networks [17] . This model reproduces the stationary dy-

namics of conductance-based networks of RS and FS cells in in AI states in stationary conditions. Nevertheless, this mean-field model (together with its protocol for TF calculation) does not consider adaptation in RS-cells and its dynamics.

It is, however, desirable to include adaptation explicitly in mean-field models for several reasons. First, adaptation strongly affects the response of cortical network to external stimuli. This was shown previously by the mismatch of the AdEx mean-field model to capture the response to transient stimuli, as well as the frequency response of the network [17] . Second, adaptation may play a role in the genesis of slow oscillatory states, such as during sleep or anesthesia, and where UP and DOWN states alternate. Indeed, computational models have shown that the progressive build-up of adaptation during UP states, and its decay during DOWN states, could account for these slow oscillations [11, 19, 20]. Although simplified models were proposed for UP-DOWN state oscillations [4, 21], there is at present no mean-field model of such adaptation dynamics derived from conductance based spiking neural network.

In this paper we introduce the dynamics of adaptation in a mean-field model of spiking networks, using a Master Equation formalism [13]. We apply this formalism to a network model of RS-FS AdEx neurons and we include adaptation in this formalism, permitting to calculate the TF of RS cells. We test the mean-field model and the effects of adaptation for network transient and stationary response to external stimuli. We report a state-dependent (depending on its ongoing activity) response of the network which arises from the interplay of low vs. high conductances and adaptation dynamics. The mean field model is able to capture such effect, taking into account both conductances and adaptation. We also investigate the emergence of UP-DOWN oscillations in the system driven by adaptation in a bistable state of the network, where a self-sustained AI state is possible if adaptation is small enough.

II. METHODS

We describe in this section the spiking network model here considered and the mean-field equations we use to compare with it.

A. Spiking network models

We consider a population of $N = 10^4$ neurons connected over a random directed network where the probability of connection between two neurons is $p = 5\%$. We consider excitatory and inhibitory neurons, with the 20% inhibitory neurons. The dynamics of each of the two types of neurons is based on the adaptive integrate and fire model described by the following equations

$$c_m \frac{dv_k}{dt} = g_L(E_L - v_k) + \Delta e^{\frac{v_k - v_{thr}}{\Delta}} - w_k + I_{syn} \quad (1)$$

$$\frac{dw_k}{dt} = -\frac{w_k}{\tau_w} + b \sum_{t_{sp}(k)} \delta(t - t_{sp}(k)) + a(v_k - E_L), \quad (2)$$

where $c_m = 150$pF is the membrane capacity, v_k is the voltage of neuron k and, whenever $v_k > v_{thr} = -50mV$ at time $t_{sp}(k)$, v_k is reset to the resting voltage $v_{rest} = -65mV$ and fixed to that value for a refractory time $T_{refr} = 5ms$. The leak term has a fixed conductance of 10nS and the leakage reversal E_L is varied in our simulations but is typically -65mV. The exponential term has a different strength for RS and FS cells, i.e. $\Delta = 2$mV ($\Delta = 0.5$mV) for excitatory (inhibitory) cells. Inhibitory neurons are modeled according to physiological insights as fast spiking FS neurons with no adaptation while excitatory regular spiking RS neurons have a lower level of excitability due to the presence of adaptation (while b varies in our simulations we fix $a = 4$nS and $\tau_w = 500$ms if not stated otherwise). The synaptic current I_{syn} received by neuron i is the result of the spiking activity of all pre-synaptic neurons $j \in \text{pre}(i)$ of neuron i. This current can be decomposed in the result received from excitatory E and inhibitory I pre-synaptic spikes $I_{syn} = (E_e - v_k)I^e_{syn} + (E_i - v_k)I^i_{syn}$, where $E_e = 0$mV ($E_i = -80$mV) is the excitatory (inhibitory) reversal potential. Notice that we consider voltage dependent conductances. Finally, we model I^e_{syn} as an decaying exponential function that takes kicks of amount Q_E at each pre-synaptic spike, i.e.:

$$I^e_{syn}(t) = Q_e \sum_{exc.pre} \delta(t - t^e_{sp}(k)) e^{-\frac{t - t^e_{sp}(k)}{\tau_e}}, \quad (3)$$

where $\tau_e = \tau_i = 5$ms is the decay time scale of excitatory and inhibitory synapses and $Q_e = 1$nS ($Q_i = 5$nS) the excitatory (inhibitory) quantal conductance. We will have the same equation with $E \to I$ for inhibitory neurons.

B. Mean-field equations

For the theoretical analysis of asynchronous dynamics in sparsely connected random networks we use the mean-field approach proposed by El Boustani & Destexhe in [13]. In this framework, based on a master equation formalism, differential equations for the population average firing rate ν_e (ν_i) of the excitatory (inhibitory) populations in the network, are derived, with a time resolution T. In fact, the main hypothesis in this formalism, consist in considering the system memoryless after a time T, or,

in other words, to consider a Markovian dynamics for the network.

In this paper we extend the model described in [13] by including the effects of adaptation. The same formalism indeed easily allows this kind of extension, as far as the time scale that drives the dynamics of the adaptation variable $w(t)$ is slow with respect to the time scale of the mean-field formalism T. It is possible to show that when a generic slow variable W (with time constant much longer than the mean-field time-scale T) is added to the system, one can close the equations for the population activities following [13] considering X as stationary at every step of the Makrovian process T (see Appendix A). When applied to the simpler case discussed in this paper of one excitatory and one inhibitory populations, with population activities $\mu = \{e, i\}$, the differential equations read:

$$
\begin{aligned}
T\partial_t \nu_\mu &= (F_\mu - \nu_\mu) + \frac{1}{2} c_{\lambda\eta} \frac{\partial^2 F_\mu}{\partial \nu_\lambda \partial \nu_\mu}, \\
T\partial_t c_{\lambda\eta} &= \delta_{\lambda\eta} \frac{F_\lambda(1/T - F_\lambda)}{N_\lambda} + (F_\lambda - \nu_\lambda)(F_\mu - \nu_\mu) \\
&\quad + \frac{\partial F_\mu}{\partial \nu_\lambda} c_{\lambda\mu} + \frac{\partial F_\mu}{\partial \nu_\eta} c_{\mu\eta} - 2c_{\lambda\mu}, \\
\partial_t W &= -\frac{W}{\tau_w} + b\nu_e. \qquad (4)
\end{aligned}
$$

where $F_{\mu=\{e,i\}} = F_{\mu=\{e,i\}}(\nu_e, \nu_i, W)$ is the transfer function of a neuron of type μ, i.e. its output firing rate excitatory and inhibitory input with rates ν_e and ν_e and with a level of adaptation W. Accordingly here the transfer function is now a function not only of the firing rate ν_e and ν_i, but also of the adaptation W.

1. *Noisy Mean field for UP-DOWN states dynamics*

In order to account for noise induced by an external drive ν_{drive} of Poissonian spike trains targeting both excitatory and inhibitory networks we consider an additive noise modeled as an Ornstein–Ulhenbeck (OU) process to Eq.s 4. Accordingly, the external drive ν_{drive} becomes here a time dependent variable $\nu_{drive}(t) = \nu_{drive} + \sigma\xi(t)$, where $\xi(t)$ is an (OU) process with a fast time scale of 5ms , $\sigma = 10.5$ is the noise amplitude and ν_{drive} is the average of the process $\nu_{drive}(t)$.

C. Neurons transfer function

We perform a semi-analytical derivation of the transfer function TF of RS and FS neurons following [17]. Here, at variance with Zerlaut et al. (2018), we take explicitly into account the effect of adaptation for the transfer function calculation as the firing rate of a single neuron depends on the input firing rate but also on the adaptation current w affecting its voltage dynamics. The method is based on the hypothesis that the output firing rate of a neuron can be written as a function of the statistics of its sub-threshold voltage dynamics, i.e. the average sub-threshold voltage μ_V, its standard deviation τ_V and its time correlation decay time τ_V.

We report first how to evaluate $(\mu_V, \sigma_V, \tau_V)$ as a function of the inputs firing rates (ν_E, ν_I) and the adaptation intensity w.

1. *From input rates to sub-threshold voltage moments*

Following [Kuhn2004], the mean membrane potential is obtained by taking the stationary solution to static conductances given by the mean synaptic bombardment with firing rates (ν_E, ν_I). We can calculate the average $\mu_{Ge,Gi}$ and standard deviation $\sigma_{Ge,Gi}$ of such bombardment for both excitatory and inhibitory process (described by Eq. (3)) in the case spikes follow a Poissonian statistics:

$$
\begin{aligned}
\mu_{Ge}(\nu_e, \nu_i) &= \nu_e\, K_e\, \tau_e\, Q_e \\
\sigma_{Ge}(\nu_e, \nu_i) &= \sqrt{\frac{\nu_e\, K_e\, \tau_e}{2}}\, Q_e \\
\mu_{Gi}(\nu_e, \nu_i) &= \nu_i\, K_i\, \tau_i\, Q_i \\
\sigma_{Gi}(\nu_e, \nu_i) &= \sqrt{\frac{\nu_i\, K_i\, \tau_i}{2}}\, Q_i,
\end{aligned} \qquad (5)
$$

The mean conductances will control the input conductance of the neuron μ_G and therefore its effective membrane time constant τ_m:

$$
\begin{aligned}
\mu_G(\nu_e, \nu_i) &= \mu_{Ge} + \mu_{Gi} + g_L \\
\tau_m(\nu_e, \nu_i) &= \frac{C_m}{\mu_G}
\end{aligned} \qquad (6)
$$

For a specific value w of the adaptation current (whose dynamics we remember to be much slower that voltage fluctuations) we obtain the following formula for the average voltage (neglecting the exponential term in Eq.(1)):

$$
\mu_V = \frac{\mu_{Ge}\, E_e + \mu_{Gi}\, E_i + g_L\, E_L - w}{\mu_G}. \qquad (7)
$$

The calculation of σ_V and of τ_V is identical to [17], we just report the final formula:

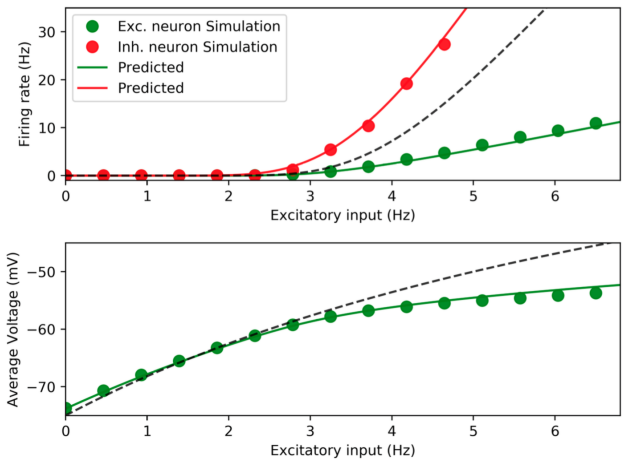

FIG. 1. **Transfer function evaluation** Top: RS (green) and FS (red) neuron stationary firing rate in function of the input excitatory firing rate ν_E for $\nu_I = 8Hz$. Dots are direct simulation and continuous line prediction based on the semi-analytical transfer function. Black dashed line is the prediction obtained neglecting adaptation in the evaluation of neuron depolarization μ_V (see lower panel). Down: RS-cell average depolarization: dots direct simulation, line prediction based on Eq. (12) and dashed line prediction neglecting adaptation. Observe the necessity of a good evaluation of μ_V to predict correctly neuron firing rate (upper panel).

$$\sigma_V(\nu_e,\nu_i) = \sqrt{\sum_s K_s\,\nu_s\,\frac{(U_s\cdot\tau_s)^2}{2\,(\tau_{\rm m}^{\rm eff}+\tau_s)}} \tag{8}$$

$$\tau_V(\nu_e,\nu_i) = \left(\frac{\sum_s\left(K_s\,\nu_s\,(U_s\cdot\tau_s)^2\right)}{\sum_s\left(K_s\,\nu_s\,(U_s\cdot\tau_s)^2/(\tau_{\rm m}^{\rm eff}+\tau_s)\right)}\right), \tag{9}$$

where we defined $U_s = \frac{Q_s}{\mu_G}(E_s-\mu_V)$.

2. *From sub-threshold voltage moments to the output firing rate*

Once calculated (μ_V,σ_V,τ_V) as a function of (ν_E,ν_I,w) we evaluate the output firing rate of a neuron according to the following formula:

$$\nu_{out} = \frac{1}{2\,\tau_V}\cdot Erfc\left(\frac{V_{thre}^{eff}-\mu_V}{\sqrt{2}\,\sigma_V}\right) \tag{10}$$

It has been shown, both theoretically and experimentally, that the voltage effective threshold V_{thre}^{eff} can be expressed as a function of (μ_V,σ_V,τ_V). In particular, the phenomenological threshold was taken as a second order polynomial in the following way:

$$V_{thre}^{eff}(\mu_V,\sigma_V,\tau_V^N) = P_0 + \sum_{x\in\{\mu_V,\sigma_V,\tau_V^N\}} P_x\cdot\left(\frac{x-x^0}{\delta x^0}\right) + \sum_{x,y\in\{\mu_V,\sigma_V,\tau_V^N\}^2} P_{xy}\cdot\left(\frac{x-x^0}{\delta x^0}\right)\left(\frac{y-y^0}{\delta y^0}\right). \tag{11}$$

We evaluated $\{P\}$ through a fit according to simulations on single neurons activity. In general, the values of $\{P\}$ do not depend on the parameters of single neuron dynamics (leakage, adaptation etc..) but we found a small dependence on the values of the neurons coupling parameters and on the parameters of the exponential term in single neuron dynamics that has been neglected in the derivation of membrane voltage moments. We perform the fit and calculate $\{P\}$ in a case without adaptation for the sake of simplicity. We will use always this values of $\{P\}$ for all the analyses performed in the paper (see table I).

The strong point of this analysis is that, once the fit is performed for a neuron with $b = 0$ and other fixed parameters, like the leakage currents, the same transfer function works also far from this fitting point because the effect of b, E_L and the other parameters is included in the theoretical evaluation of (μ_V,σ_V,τ_V) whose values define the neuron output firing rate. In principle, the fit could be performed for any values of the parameters.

Let us notice that, for the sake of comparison, a slightly different approach was used in Zerlaut et al. 2018. In this case the adaptation current was neglected and thus the parameters of the fit $\{P\}$ where adjusted to take into account the approximation in the derivation of μ_V. Accordingly, in that case the fit changes changing the parameters of the neuronal model like adaptation parameters (b and a) and the fit has to be performed for any model parameters values in order to have a reliable transfer function.

In Fig. 1 we show the result of the procedure here adopted for the evaluation of the transfer function. We consider RS-cell with a relatively high adaptation ($a = 4$, $b = 20$). We observe that this method is able to capture both neurons firing rate (upper panel) and their average voltage (lower panel). Moreover, we notice that not considering adaptation in the calculation of μ_V overestimates RS-cell voltage and would lead to a dramatic discordance for neuron firing rate (see black dashed line). In the methodology we use here we estimate the average voltage calculating adaptation in its stationary state, yielding the following result:

$$\mu_V = \frac{\mu_{Ge}\,E_e + \mu_{Gi}\,E_i + g_L\,E_L - \nu_{out}\tau_w b + aE_L}{\mu_G + a}, \tag{12}$$

where ν_{out} is the predicted firing rate of the neuron according to the transfer function.

TABLE I. **Fit parameters (expressed in mV)**

Cell type	P_0	P_1	P_2	P_3	P_4	P_5	P_6	P_7	P_8	P_9
RS–cell	-49.8	5.06	-25	1.4	-0.41	10.5	-36	7.4	1.2	-40.7
FS–cell	-51.4	4.0	-8.3	0.2	-0.5	1.4	-14.6	4.5	2.8	-15.3

III. RESULTS

Equipped with the formalism developed in the previous section, we can now analyze the results provided by the mean-field and compare them to the simulated neural network dynamics. We performed this analyses focusing on the response to various time-dependent input stimuli and by exploring different directions in the parameters space (adaptation strength, neurons excitability etc..).

A. Network spontaneous activity and mean-field prediction

We started by considering a region in the parameters space in which an excitatory external drive $\nu_{drive} > 0$ is necessary in order to have spiking activity in the network. This corresponds, as we will see later, to choose low excitability level (low leakage reversal) for RS cells, i.e. $E_L^E = E_L^I = -65$mV. We chose $\nu_{ext} = 2.5$Hz, which guarantees an asynchronous irregular (AI) network dynamics with physiological values of conductances and neuron firing rates. As a first step we investigated the effect of adaptation on the spontaneous activity of the network, verifying the prediction capability of the mean-field model, focusing on the role of the adaptation strength b.

We report in Fig. 2 the result of a network simulation, recording the average firing rate ν_e and ν_i of excitatory and inhibitory neurons (Fig. 2A) as well as the average voltage (averages are intended over time and over all neurons of the same type) μ_V (Fig. 2B). By increasing adaptation strength b we observe, as expected, a decrease in both excitatory and inhibitory firing rates (panel A, respectively green and red dots), accompanied by a decrease in μ_V (panel B, blue dots).

These quantities can be calculated from the mean-field model with adaptation described in Sec. II. The average voltage μ_V is obtained from Eq. (12). In the same figure, we compare the simulation results with those of the mean-field model for the firing rates of the population (green and red solid lines in Fig. 2A for excitatory and inhibitory populations) and for the membrane potential (blue solid line in Fig. 2B). In the insets we report the comparison between the distribution of values in simulations and the theoretical results in the mean-field, for the specific parameter value $b = 60$nS. We observe that the mean-field is able to capture the spontaneous activity of the network and its fluctuations. It is worth notice that the spontaneous activity of the network could have been captured also with a 'naive' version of this mean-field model considering only stationary values of adaptation and not its time dynamics (for the sake of simplicity we refer to this version of the mean-field model as "stationary"). Nevertheless, in order to obtain a good mean-field estimation of neurons average voltage of Fig. 2B, one always needs to take into account the adaptation effects (see Fig. 1 in Sec. II).

B. Response to external stimuli

Even if the spontaneous activity of the populations firing rate in the network could be sufficiently well predicted also by using a "stationary" mean-field, in this section we will show how adaptation dynamics needs to be taken into account when the stationarity condition is not satisfied[22]. In particular we studied the response of the network to time-dependent external stimuli. We report in Fig. 3 (A1-A3) three different examples of external stimuli:

- In Fig 3-A1 we add an extra stimulus ν_{ext} with exponential rise and decay, to the external drive. If the rise and decay time scales are smaller than the time scale of the adaptation dynamics (as it is usually the case, since adaptation is a slow variable – $\tau_w = 500$ms in our case) only a mean-field model taking W into account can predict the network response in a correct way. By looking at the comparison between a mean-field model with or without adaptation (green vs. blue line) we observe that the extended version of the mean-field correctly captures the first peak of response, as well as an hyper-polarization at the stimulus offset due to the accumulation of adaptation.

- In Fig. 3-A2 we consider a input yielding an inhibition by temporarily turning off the initially constant external drive ν_{drive}. We observe a rebound response captured very well in its time course by the mean-field model. The effect of adaptation is therefore very strong also by looking at the network response after inhibition.

- In Fig 3-A3 we show the response to an oscillatory input of a fixed frequency f_{inp}. It is evident how the effect of adaptation allows the mean-field to catch the time-dependent amplitude of the response, while it is always constant and underestimated in the naive case of "stationary" mean-

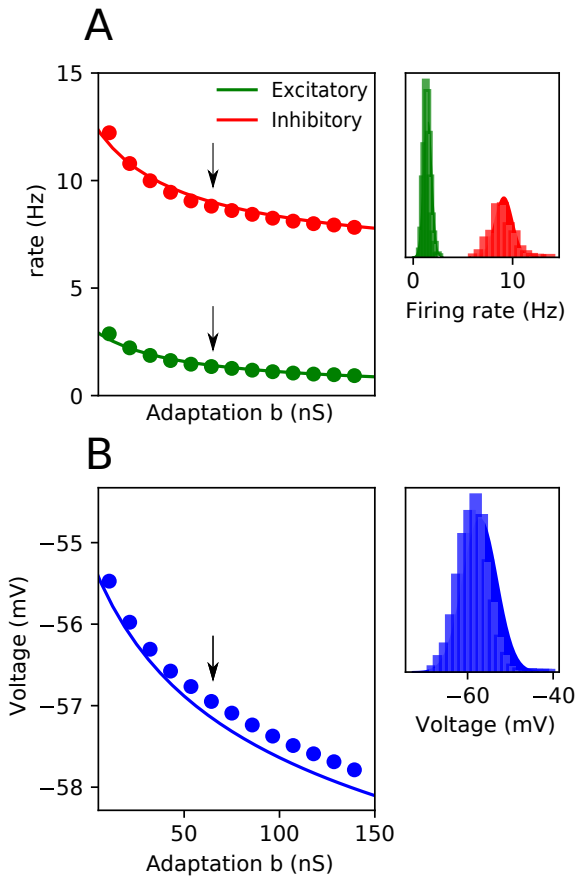

FIG. 2. **Spontaneous activity. Panel A**: average firing rate from spiking network simulation. Solid lines are the means predicted by the mean-field model. In the right inset we report the firing rate distribution sampled from the spiking simulation (histogram) and the theoretically predicted Gaussian distribution (shading), for $b = 60$nS. Green and red are consistently referred to excitatory and inhibitory neurons. **Panel B** (Dots) average membrane potential from spiking simulation and (line) theoretical prediction. Inset, membrane potential distribution sampled from spiking simulation (histogram) and theoretically predicted distribution (shading), for the excitatory neurons for $b = 60$nS.

field. Adaptation dynamics is then responsible for network increased response to an oscillating external input ν_{ext}.

In Fig. 3D we study more extensively the response of the network to oscillating external inputs, as a function of f_{inp}. In particular, we show that the amplitude of the oscillations of the firing rate (the difference between the maximum and the minimum firing rate once the system has passed the transient phase) in the network simulations has a very non-trivial behavior when the frequency varies. First, there is an increase at $f_{inp} \sim 2$Hz. Then, a resonance peak appears around 10-50 Hz [17]. Finally, a maximum peak is followed by a drop at a second time scale around $f_{inp} \sim 20$Hz. The mean-field is able to capture these combined effects and gives us an indication on their origin. The rise observed at $f_{inp} \sim 0.2$Hz can be related to the time scale of adaptation $\tau_w \sim 1/f_{inp}$. In fact, without adaptation, the mean-field (blue line of Fig. 3D) does not show the same increase at low frequencies and instead it is completely transparent to the frequency of the external input, until the resonance peak. In fact, given the relatively high strength (compared to the external input) of the excitatory-inhibitory loop, the system is close to a bifurcation toward oscillations ([23]) and when forced at the correct frequency, the response is amplified ([24]). This is the case for both models, with or without adaptation. Finally, the decay from the baseline response amplitude appears at frequencies of order $1/T$ and can be easily understood by observing that when the stimulus varies faster than the correlation time scale of the mean-field, it appears as an effective constant external drive and the oscillations disappear. Consistently, the same decay at high frequencies is conserved in the "stationary" mean-field.

C. State-dependent responsiveness

We study in this section the response of the network as a function of its dynamical state preceding the input arrival. The input here considered corresponds to one cycle of a sinusoidal wave of spike train at a frequency $f = 5Hz$ (see insets in Fig. 4). We study two different parameter setups that differ for the baseline drive the system receives. In case (A) $\nu_{drive} = 7Hz$ and the system sets in an asynchronous state with relatively high firing rate and very high conductance level ($G_E/G_l \sim 3$) while in case (B) $\nu_{drive} = 1.5Hz$ and neurons firing rates are lower and conductance state has realistic values ($G_E/G_l \sim 0.8$). We observe that, for the same stimuli, network (B) has a much greater response to the input with respect to network (A). Moreover, the mean field model is able to capture this difference and gives a very good prediction of response time course. This effect is even stronger when comparing the relative response of the two networks with respect to their baseline (see in Fig. 4C the comparison between the two continuous lines). The state-dependent responsiveness of the system is a combination of two effects: the dynamics of adaptation and the conductance state. In order to elucidate this mechanism we report in Fig. 4C (dashed lines) the responses in the "stationary" model, as done in Fig 3. We observe that such model does not capture the right peak in response to the stimuli. In fact, the peak is strongly affected by the level of adaptation pre-stimulus, which is quite low as the excitatory neurons firing rate is low. Accordingly, when a sufficiently fast stimuli (with respect to the time scale of adaptation, as it is the case for 5Hz) is presented, the system will strongly activate. The dynamics of adaptation

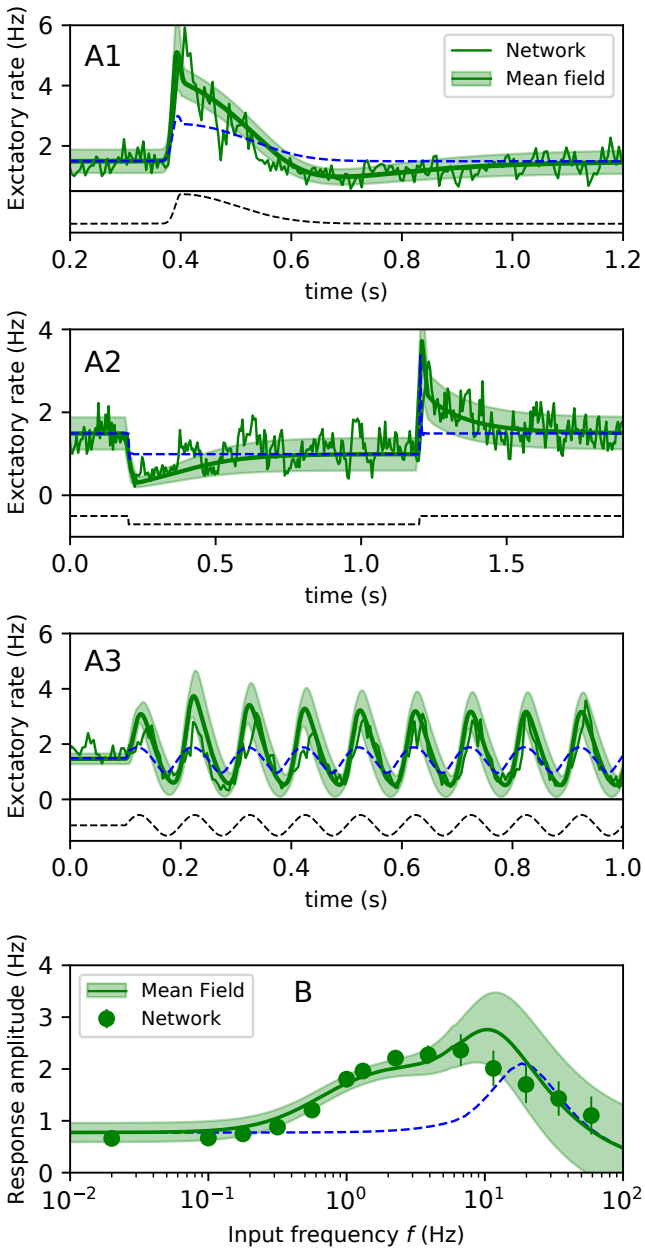

FIG. 3. **Response to external stimuli. A1-3** Population activity of the excitatory sub-populations in presence of different time-varying external stimuli (green). Superimposed is the mean and standard deviation over time predicted by the Markovian formalism. (bottom) Time-course of the external stimulus. (blue) The theoretical prediction when the adaptation variable W is fixed to its stationary value $\bar{W} = \tau_w * b * \nu_E$. **B** (Dots) Amplitude of network oscillations, in response to an oscillating input as a function of the input frequency. Superimposed is the mean and standard deviation predicted by the model. (blue) The theoretical prediction when the adaptation variable W is fixed to its stationary value $\bar{W} = \tau_w * b * \nu_E$.The parameter a is set to zero in these simulations.

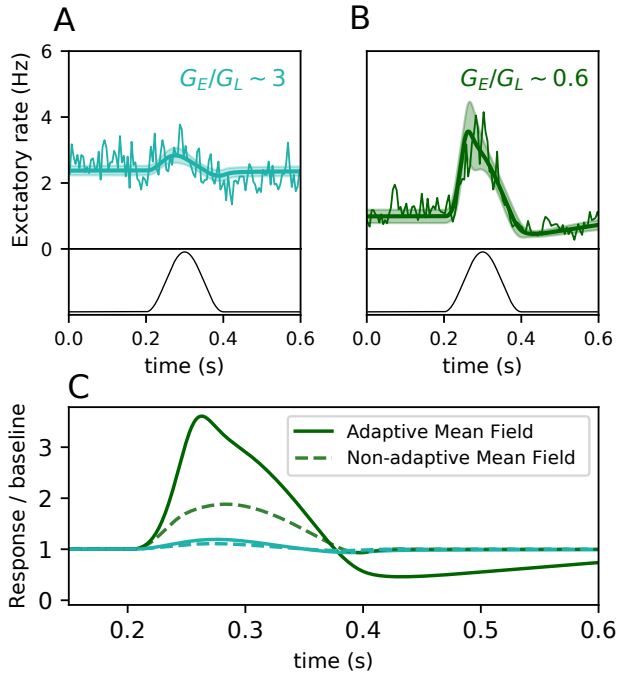

FIG. 4. **State-dependent response.** Population activity of the excitatory sub-populations in presence in response to a cycle of a sinusoidal input of amplitude 2Hz. Superimposed is the mean and standard deviation over time predicted by the Markovian formalism. Green dark color (right panel) has a different baseline firing rate with respect to light cyan (left panel) due a different ν_{drive} (ν_{drive} = 1.5Hz for green and ν_{drive} = 7Hz for cyan). The dashed line correspond to the mean field model where adaptation is not evolving in time but takes values corresponding to its stationary value (as in Fig 3).

is thus responsible for a good part of the state dependent response, due to the lower or higher pre-stimuli adaptation/excitatory neurons firing rate. On the other hand, also a model that does not take into account the time evolution dynamics of adaptation (dashed line) shows an increased responsiveness in the lower conductance state. This shows the importance of using a mean-field model taking into account both conductances and adaptation dynamics.

D. Transition to self-sustained bistable network activity

In the setup used so far, the network needs a constant external drive ν_{drive} in order to be set in an AI state. In the absence of external drive, $\nu_{drive} = 0$, the only stable state of the system is silent, with $\nu_e = \nu_I = 0$. This is true for the case we investigate here of adaptation set to zero. We will reintroduce adaptation in next section to study its effects. We show in Fig.5 that it is possible

to observe a transition to a bistable network, by modifying the excitability of RS and FS cells. This is done by changing the resting potential (actually changing the leakage reversal potentials E_L^E and E_L^I). In order to verify the existence of a bistable network dynamics in the spiking network we perform a simulation with an initial kick ($\nu_{drive} = 1$ Hz) applied to the network for a small period of time (around 100 ms). In the case of a bistable system the network activity rises and then remains to a non-zero firing rates, even after the end of the stimulus. On the contrary, the system will come back at some point to a silent state. We report in the inset of Fig.5B the two cases (i) $E_L^E = -67\text{mV}, E_L^I = -65\text{mV}$ (red triangle) and (ii) $E_L^E = -63\text{mV}, E_L^I = -65\text{mV}$ (green square). By plotting the firing rates average after the stimulus offset (we measure for 5s starting 1s after the stimulus offset) as a function of E_L^E and E_L^I, we observe the existence of a clear transition line separating a bistable regime to a state with only one silent stable state Fig.5A. The bistability regime is achieved as soon as the excitability of RS cells overcomes the excitability of FS cells by a certain amount. In particular, the transition line (the couples of critical points $(E_{L,c}^E, E_{L,c}^I)$) lies almost at the bisector of the square, meaning that the critical point is achieved at the critical ratio $R_c = E_{L,c}^E / E_{L,c}^I \sim 1$.

The existence of two stable fixed points in the network dynamics can be then investigated in the mean-field model. We report in Fig5B a graphical solution for the fixed point of ν_e. It is calculated as follows. We scan the values of ν_e (x-axes) and we calculate the corresponding $\bar{\nu_I} = T_{FS}(\nu_e, \bar{\nu_I})$ (1st order mean-field $\dot{\nu_I} = 0$). We then calculate the corresponding $\mathcal{F}(\nu_e) = T_{RS}(\nu_e, \bar{\nu_I})$. We obtain a fixed point of the system when $\mathcal{F}(\nu_e) = \nu_e$. We thus plot the function $\mathcal{F}$ and search for intersection with the bisector. Let us consider the case (i) (see heat plot in Fig5A) which corresponds to parameters for which in the network we observe only one silent stable state. We observe that actually the mean-field predicts correctly that there is only one intersection at $\nu_e = 0$. Let us notice, for the sake of completeness, that it exists always a couple of other fixed point not shown in the plot at very high frequencies (one stable and one unstable), corresponding to the unrealistic case $\nu_e = \nu_I = 1/T_{refr}$. Increasing the excitability of RS cells (case (ii)) we observe the appearance of two new fixed points. We verified that the higher in firing rates is indeed stable. We then superimpose the firing rate of the network after a kick for these values of the leakage, and we observe that actually the mean field fixed point matches with network simulations. Using this method we are able to calculate the transition curve from a self-sustained to a non-self-sustained regime in function of E_L^E and E_L^I, that we superimpose in the spiking network simulations reported in the heat-plot of Fig. 5A, finding a very good agreement.

Let us notice that, again, even if the fit for the transfer function (see methods) has been done for a specific value of E_L^E and E_L^I, it still gives correct results also moving around in the parameter space.

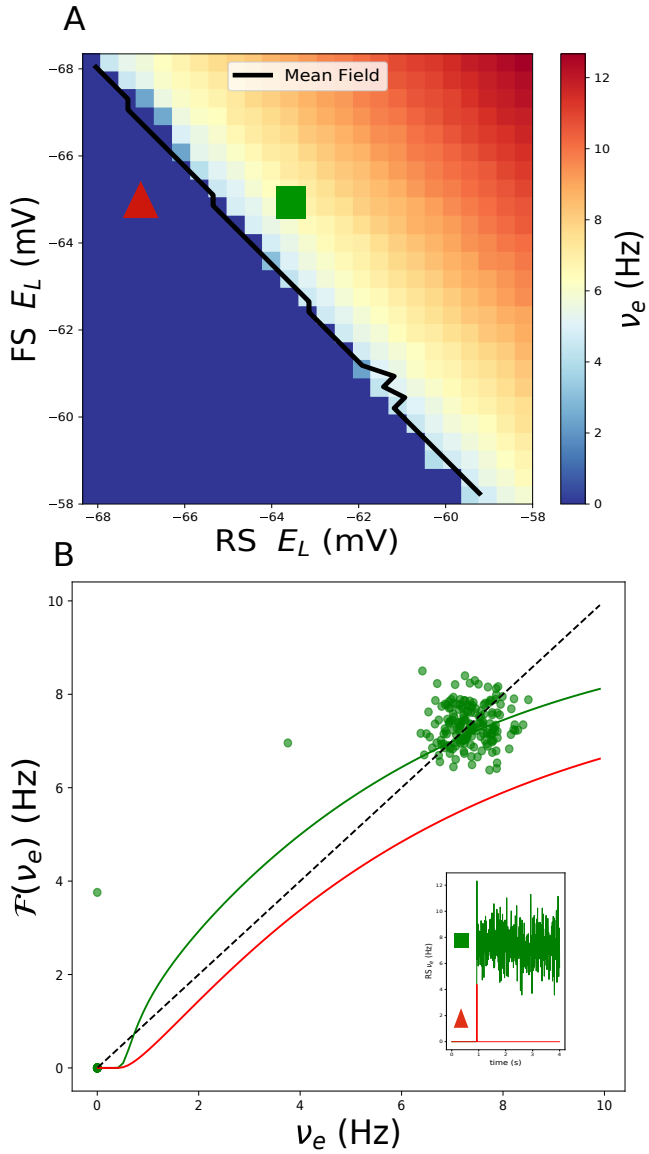

FIG. 5. **Transition to self-sustained activity** A: Firing rate of excitatory neurons (averaged over 5s) after the kick of duration of 100ms. The black line is the prediction from mean field for the transition point. B: Function $\mathcal{F}$ derived by mean-field equations in the two cases (green and red curves). The dashed black line is the bisector. In the inset the excitatory response of the network to the kick in two cases ($E_L^I = -63mV$ and $E_L^E = -67mV$). Green light dots in the main panel have been obtained from the network simulation shown in the inset.

Moreover, we point out that this self-sustained regime is characterized by physiological conductances, observing a quite large range of parameter values where the conductances stay at a physiological value, at variance with other models present in the literature ([10]).

E. UP-DOWN states dynamics triggered by noise and adaptation

We report here the effects of adaptation on the network dynamics in the case of a bistable system (case (ii) of the previous section). In the absence of any external drive the system has still the same dynamics as in the case without adaptation, i.e. silent or self-sustained state. Nevertheless, this state is less stable the more the adaptation strength increases. We consider $b = 60$ nS, yielding a realistic level of adaptation to RS cells. For this parameter value the active state is unstable and only a silent state is permitted.

As soon as a small external drive is added to the system (here we use $\nu_{drive} = 0.315$ Hz), it introduces a noisy level of activity in the silent (down) state. As in the down state adaptation is almost zero, the second "active" state is stable. Accordingly, noise permits to the system to "jump" to the active (UP) state. Nevertheless, as adaptation grows (because of neurons firing), the UP state loses stability and the network goes back to the DOWN state (see Fig. 6). The duration of the UP state is related to the speed at which adaptation grows as function of the neurons firing rate increase. Nevertheless, we observe that UP state durations are heterogeneous and characterized by "bumps" of activity, revealing a non-trivial dynamical structure that is induced by finite size noise fluctuations. The alternation of UP states is irregular, as their duration and structure. Moreover the conductances of the system stay in a physiological range, as expected by previous analyses (Fig5).

The deterministic mean-field model with adaptation used until now cannot reproduce this kind of dynamic as it does not take into account the amount of noise induced by non-zero external drive ($\nu_{drive} = 0.315$ Hz). As this external drive is a Poissonian train of spikes, we added a noisy term $\xi(t)$ as an OU process with fast time decay (5ms, see methods for details) to the mean field equations. A simulation of the mean-field model in this set-up is reported in Fig.7. We observe the alternation of silent periods with transients of high activity. The firing rates during the UP states are quantitatively matching those of the spiking network simulations, as their duration Finally, a certain level of heterogeneity in between UP states is reproduced by the mean field, where rebounds of activity are present, exactly as in spiking network simulations. In Fig.7B we superimpose the network dynamics during an UP-DOWN cycle to the activity map derived for the mean field (like done in Fig5B). We observe that the trajectory drawn by the network follows the stability principles dictated by the mean field. The system is dynamically bistable when adaptation in zero (DOWN state) and can jump to the UP state. Then, when adaptation builds up, the system is not bistable anymore and comes back to the DOWN state.

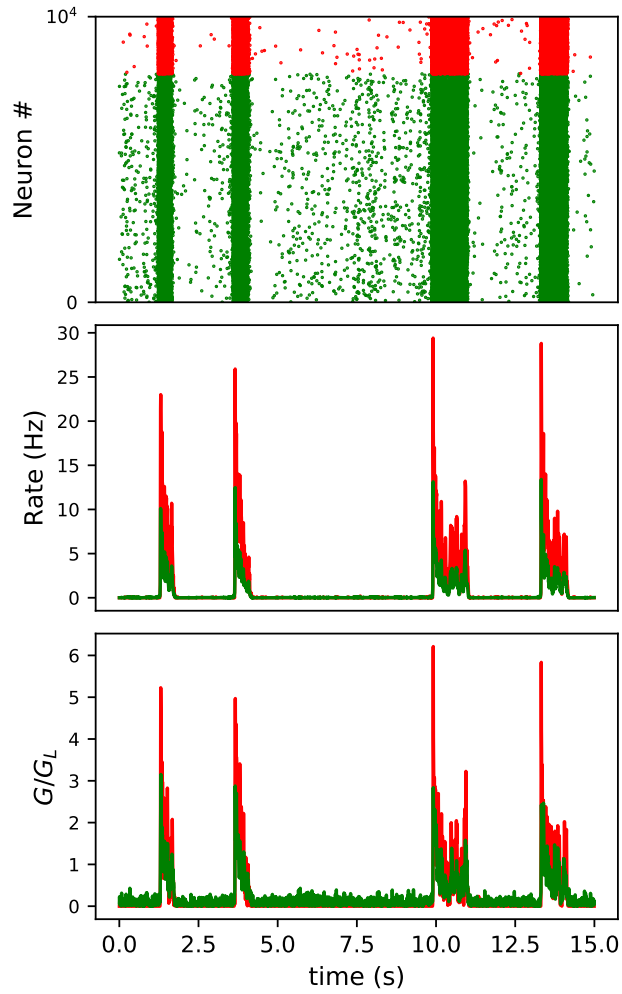

FIG. 6. **UP DOWN state in bistable network** From top to down: raster plot, neurons firing rate and conductances rescaled with the leakage g_L. A little amount of the external poissonian spikes $\nu_{ext} = 0.315$ Hz are provided to the network. The value of RS-cell leak $E_L = -63mV$.

IV. CONCLUSIONS

We studied a dynamical mean field model of a conductance–based network of Adaptive Exponential integrate and fire neurons. We used an extended version of a master equation formalism in order to take into account slow variables like adaptation, taking into account the memory of the network dynamics, not considered in the original Markovian formulation [13]. Even if we used a fitting approach for the calculation of the transfer function for one set of model parameters this approach turned out to be satisfying and quite robust with respect

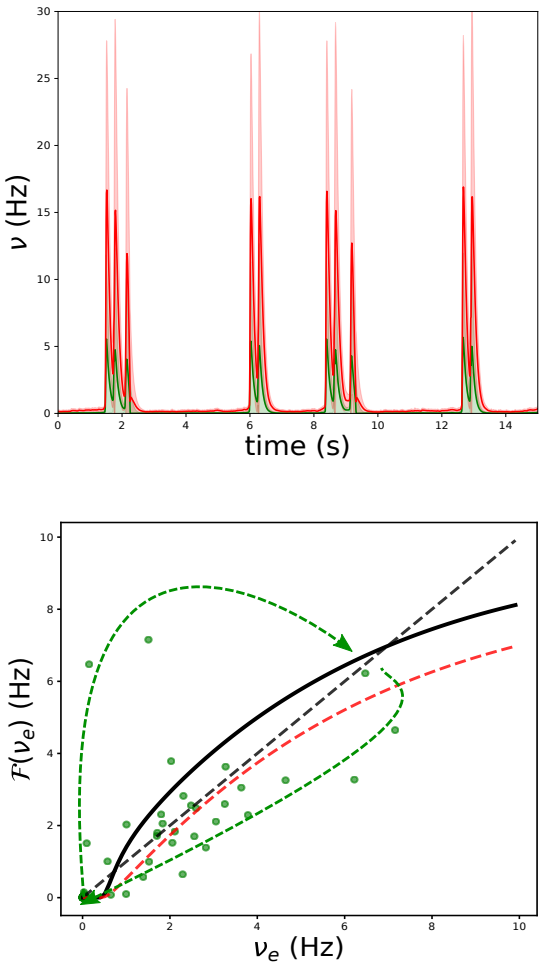

FIG. 7. **Adaptation and UP DOWN state in bistable mean field model** Dynamics of the mean field model with the parameters of the network of Fig. 6 (RS $E_L = -63mV$ and $\nu_{ext} = 0.315$). Top: neurons firing rate (green for excitation and red for inhibition), shadows represent the covariance based on second order mean field evaluations. Bottom: Phase plane derived from mean field with superimposed the firing rate (green dots) of the network dynamics (Fig. 6). Black line is relative to the transfer function for $E_L = -63mV$ (zero adaptation) and blue dashed line is relative to a lower leakage reversal due to adaptation building up during the UP state. Green dashed line is used to guide the eyes through the spiking network trajectory during DOWN-UP cycle.

to parameters change. In fact, as adaptation varies dynamically (e.g. during UP-DOWN state dynamics) or as neurons parameters change (e.g. neurons leakage), the mean field model gives good predictions even far from the benchmark point where the fitting has been done. This confirms that, in the dynamical regimes investigated here, the hypothesis that the neuron firing rate can be expressed as a function of neuron sub-threshold voltage statistics is correct, and yields good predictions as far as those quantities (μ_V, σ_V and τ_V) are accurately calculated (e.g. taking into account adaptation). While the formalism used here has been applied to spike frequency adaptation, it could potentially be used for other purposes, e.g. other external variables like Spike-Time-Dependent-Plasticity (STDP), capable to yield different dynamical regimes with respect to those investigated here ([25]) or synaptic dynamics in general. Moreover, the approach we used to calculate the transfer function is very general and it may be applied to other neuronal models or to real data ([18]), provided the neuron dynamics has a stationary firing rate (e.g. this approach should be changed if one take into account other neuronal mechanism like bursting [26]). Interestingly, in [18] it has been shown that neurons are highly heterogeneous, as reported also by [15], where the parameters of adaptation dynamics strongly vary across neurons. In the present mean field model formulation, neuronal heterogeneity is not taken into account and might represent a future development of this work, to obtain a mean field model based on experimental measures. Finally, the state dependent response reported here is a result of both conductances and adaptation dynamics: This mean field approach provided a unique tool to investigate its origin and may be exploited to compare model prediction with experimental measurements.

ACKNOWLEDGEMENTS

We acknowledge funding from the European Union (Human Brain Project H2020–720270 and H2020–785907). We thank Yann Zerlaut for useful discussion.

[1] N. Dehghani, A. Peyrache, B. Telenczuk, M. Le Van Quyen, E. Halgren, S. S. Cash, N. G. Hatsopoulos, and A. Destexhe, "Dynamic balance of excitation and inhibition in human and monkey neocortex," *Scientific reports*, vol. 6, p. 23176, 2016.

[2] A. Renart, J. De La Rocha, P. Bartho, L. Hollender, N. Parga, A. Reyes, and K. D. Harris, "The asynchronous state in cortical circuits," *science*, vol. 327, no. 5965, pp. 587–590, 2010.

[3] M. V. Sanchez-Vives and D. A. McCormick, "Cellular and network mechanisms of rhythmic recurrent activity in neocortex," *Nature neuroscience*, vol. 3, no. 10, p. 1027, 2000.

[4] D. Jercog, A. Roxin, P. Bartho, A. Luczak, A. Compte, and J. de la Rocha, "Up-down cortical dynamics reflect state transitions in a bistable network," *eLife*, vol. 6, 2017.

[5] M. Sanchez-Vives and M. Mattia, "Slow wave activity as the default mode of the cerebral cortex," *Arch. Ital. Biol*, vol. 152, no. 2-3, pp. 147–155, 2014.

[6] M. Steriade, I. Timofeev, and F. Grenier, "Natural waking and sleep states: a view from inside neocortical neurons," *Journal of neurophysiology*, vol. 85, no. 5, pp. 1969–1985, 2001.

[7] A. Destexhe, M. Rudolph, and D. Paré, "The high-conductance state of neocortical neurons in vivo," *Nature reviews neuroscience*, vol. 4, no. 9, p. 739, 2003.

[8] S. Denève and C. K. Machens, "Efficient codes and balanced networks," *Nature neuroscience*, vol. 19, no. 3, p. 375, 2016.

[9] Y. Zerlaut and A. Destexhe, "Enhanced responsiveness and low-level awareness in stochastic network states," *Neuron*, vol. 94, no. 5, pp. 1002–1009, 2017.

[10] T. P. Vogels and L. F. Abbott, "Signal propagation and logic gating in networks of integrate-and-fire neurons," *Journal of neuroscience*, vol. 25, no. 46, pp. 10786–10795, 2005.

[11] A. Destexhe, "Self-sustained asynchronous irregular states and up–down states in thalamic, cortical and thalamocortical networks of nonlinear integrate-and-fire neurons," *Journal of computational neuroscience*, vol. 27, no. 3, p. 493, 2009.

[12] O. Shriki, D. Hansel, and H. Sompolinsky, "Rate models for conductance-based cortical neuronal networks," *Neural computation*, vol. 15, no. 8, pp. 1809–1841, 2003.

[13] S. El Boustani and A. Destexhe, "A master equation formalism for macroscopic modeling of asynchronous irregular activity states," *Neural computation*, vol. 21, no. 1, pp. 46–100, 2009.

[14] B. W. Connors and M. J. Gutnick, "Intrinsic firing patterns of diverse neocortical neurons," *Trends in neurosciences*, vol. 13, no. 3, pp. 99–104, 1990.

[15] M. Pospischil, M. Toledo-Rodriguez, C. Monier, Z. Piwkowska, T. Bal, Y. Frégnac, H. Markram, and A. Destexhe, "Minimal hodgkin–huxley type models for different classes of cortical and thalamic neurons," *Biological cybernetics*, vol. 99, no. 4-5, pp. 427–441, 2008.

[16] R. Brette and W. Gerstner, "Adaptive exponential integrate-and-fire model as an effective description of neuronal activity," *Journal of neurophysiology*, vol. 94, no. 5, pp. 3637–3642, 2005.

[17] Y. Zerlaut, S. Chemla, F. Chavane, and A. Destexhe, "Modeling mesoscopic cortical dynamics using a mean-field model of conductance-based networks of adaptive exponential integrate-and-fire neurons," *Journal of computational neuroscience*, vol. 44, no. 1, pp. 45–61, 2018.

[18] Y. Zerlaut, B. Teleńczuk, C. Deleuze, T. Bal, G. Ouanounou, and A. Destexhe, "Heterogeneous firing rate response of mouse layer v pyramidal neurons in the fluctuation-driven regime," *The Journal of physiology*, vol. 594, no. 13, pp. 3791–3808, 2016.

[19] A. Compte, M. V. Sanchez-Vives, D. A. McCormick, and X.-J. Wang, "Cellular and network mechanisms of slow oscillatory activity (¡ 1 hz) and wave propagations in a cortical network model," *Journal of neurophysiology*, vol. 89, no. 5, pp. 2707–2725, 2003.

[20] M. Bazhenov, I. Timofeev, M. Steriade, and T. J. Sejnowski, "Model of thalamocortical slow-wave sleep oscillations and transitions to activated states," *Journal of neuroscience*, vol. 22, no. 19, pp. 8691–8704, 2002.

[21] C. Capone, B. Rebollo, A. Muñoz, X. Illa, P. Del Giudice, M. V. Sanchez-Vives, and M. Mattia, "Slow waves in cortical slices: How spontaneous activity is shaped by laminar structure," *Cerebral Cortex*, pp. 1–17, 2017.

[22] Notice that in the case of time-dependent external stimuli, the value of adaptation in the.

[23] N. Brunel and X.-J. Wang, "What determines the frequency of fast network oscillations with irregular neural discharges? i. synaptic dynamics and excitation-inhibition balance," *Journal of neurophysiology*, vol. 90, no. 1, pp. 415–430, 2003.

[24] E. Ledoux and N. Brunel, "Dynamics of networks of excitatory and inhibitory neurons in response to time-dependent inputs," *Frontiers in computational neuroscience*, vol. 5, p. 25, 2011.

[25] M. Tsodyks, K. Pawelzik, and H. Markram, "Neural networks with dynamic synapses," *Neural computation*, vol. 10, no. 4, pp. 821–835, 1998.

[26] E. M. Izhikevich, "Simple model of spiking neurons," *IEEE Transactions on neural networks*, vol. 14, no. 6, pp. 1569–1572, 2003.

Appendix A: Master equation formulation in presence of slow variable.

We extend here the framework discussed in [13] using a consistent notations. Let us consider a network with K homogeneous populations of neurons. Each population γ is defined by its network activity m_γ that is the number of neurons which fired in that population in a time bin T. In the wit of making a probabilistic Markovian formulation, T should be chosen of the time-scale of correlation decay in order to have the system that only depends on the previous step. Also T should be small enough to avoid to have the same neuron firing twice in the same bin.

We also define the variable $W_\gamma = (1/N_\gamma)\sum_i w_{\gamma,i}$, where $w_{\gamma,i}$ is the adaptation of the $i-th$ neuron in population γ, as defined in the previous paragraph. The dynamics of the variables W is assumed to be slow with respect to the autocorrelation time of the system T.

We make the assumption that the state of the system is defined by the set of variables $\{m_\gamma, W_\gamma\}$. The network behavior can be investigated bu studying the transition probability $P_T(\{m_\gamma, W_\gamma\}|\{m'_\gamma, W'_\gamma\})$, i.e. the probability that the system is in $\{m_\gamma, W_\gamma\}$ at time t_0+T conditioned to the fact that it was at $\{m'_\gamma, W'_\gamma\}$ at a generic time t_0. Provided the choice for T we discussed above, we can reasonably assume that population-conditional probabilities are independent beyond the time scale of T, thus allowing to write:

$$P_T(\{m_\gamma, W_\gamma\}|\{m'_\gamma, W'_\gamma\}) = \prod_{\alpha=1..K} P_T(m_\alpha, W_\alpha|\{m'_\gamma, W'_\gamma\}) \tag{A1}$$

We can thus define the transition operator W as:

$$\mathcal{W}(\{m_\gamma, W_\gamma\}|\{m'_\gamma, W'_\gamma\}) = \frac{\prod_{\alpha=1..K} P_T(m_\alpha, W_\alpha|\{m'_\gamma, W'_\gamma\})}{T}, \tag{A2}$$

For this approximation to be valid, the time constant $\tau_w \gg T$, namely we assumed that the adaptation dynamics is slower than the firing rate dynamics.

This also involves that W variables are independent on fluctuations in firing rates and can be described by a deterministic equation. Thus the probabilities can be factorized as follows

$$P_T(\{m_\gamma, W_\gamma\}|\{m'_\gamma, W'_\gamma\}) = \bar{P}_T(\{m_\gamma\}|\{m'_\gamma, W'_\gamma\}) \cdot\delta(W_\gamma - [W'_\gamma + \frac{T}{\tau_w} f(W'_\gamma, m'_\gamma)]).$$

where we used Eulero integration for W dynamics that for linear $f()$ can be explicitly written in the following closed form

$$\partial_t \langle W_\mu \rangle = -\frac{\langle W_\mu \rangle}{\tau_w} + b\langle m_\mu \rangle. \tag{A3}$$

Using the same approach as in [13] we obtain the following equations for the average activity and for the correlations

$$\partial_t \langle m_\mu \rangle = \bar{a}_\mu(\{\langle m_\gamma \rangle, \langle W_\gamma \rangle\}) + \frac{1}{2}\partial_\lambda \partial_\eta \bar{a}_\mu(\{\langle m_\gamma \rangle, \langle W_\gamma \rangle\}) c_{\lambda\eta}$$
$$\partial_t c_{\mu\nu} = \bar{a}_{\mu\nu}(\{\langle m_\gamma \rangle, \langle W_\gamma \rangle\}) + \partial_\lambda \bar{a}_\mu(\{\langle m_\gamma \rangle, \langle W_\gamma \rangle\}) c_{\nu\lambda} + \partial_\lambda \bar{a}_\nu(\{\langle m_\gamma \rangle, \langle W_\gamma \rangle\}) c_{\mu\lambda}$$

where

$$\bar{a}_\mu(\{\langle m_\gamma \rangle, \langle W_\gamma \rangle\}) = \prod_{\beta,=1..K} \int_0^{T^{-1}} \int_\Omega dm'_\beta dW'_\beta (m'_\mu - \langle m_\mu \rangle) \mathcal{W}(\{m'_\gamma, W'_\gamma\}|\{m_\gamma, W_\gamma\}).$$

and

$$\bar{a}_{\mu\nu}(\{\langle m_\gamma \rangle, \langle W_\gamma \rangle\}) = \prod_{\beta,=1..K} \int_0^{T^{-1}} \int_\Omega dm'_\beta dW'_\beta (m'_\mu - \langle m_\mu \rangle)(m'_\nu - \langle m_\nu \rangle) \mathcal{W}(\{m'_\gamma, W'_\gamma\}|\{m_\gamma, W_\gamma\}).$$

Using the assumption made in eq.(A3) $\mathcal{W}$ can be explicitly written as

$$\mathcal{W}(\{m_\gamma, W_\gamma\}|\{m'_\gamma, W'_\gamma\}) = \frac{1}{T}\sqrt{\frac{det(A)}{2\pi^K}} \exp\left[-\frac{1}{2}(m_\mu - \nu_\mu(m'_\gamma, W'_\gamma)) A_{\mu\nu}(m_\nu - \nu_\nu(m'_\gamma, W'_\gamma)) \right] \cdot\delta(W_\gamma - [W'_\gamma + \frac{T}{\tau_x} f(W'_\gamma, m'_\gamma)]), \tag{A4}$$

where ν_μ depends on the single neuron model and where $A_{\mu\nu} = \delta_{\mu\nu} \frac{N_\mu}{\nu_\mu(m'_\gamma, W'_\gamma)(1/T - \nu_\nu(m'_\gamma, W'_\gamma)}$.

We finally get the equations for the moments:

$$T\partial_t \langle m_\mu \rangle = (\nu_\mu - \langle m_\mu \rangle) + \frac{1}{2}\partial_\lambda \partial_\eta c_{\lambda\eta}$$
$$T\partial_t \langle c_{\mu\nu} \rangle = \delta_{\mu\nu} A^{-1}_{\mu\mu} + (\nu_\mu - \langle m_\mu \rangle)(\nu_\nu - \langle m_\nu \rangle) + \partial_\lambda \nu_\mu c_{\nu\mu} + \partial_\lambda \nu_\nu c_{\nu\lambda} - 2c_{\mu\nu}$$
$$\partial_t \langle W_\mu \rangle = -\frac{\langle W_\mu \rangle}{\tau_w} + b\langle m_\mu \rangle$$

where, once again, only the first order for the equation of W are considered, since we suppose its dynamics not to be fluctuation driven. Here we stress that the activity variables dynamics are a function of the adaptation level.